Non-Markovian correlation spectra and quantum stochastic trajectory analysis of spontaneous emission of an excited two-level atom

Chang-qi Cao,* Wei Long, and Jikun Wei[†]

Department of Physics, Peking University, Beijing 100871, China

Hui Cao[‡]

Department of Physics and Astronomy, Northwestern University, Evanston, Illinois 60208-3112

The non-Markovian correlation spectra of spontaneous emission of an excited two-level atom are derived including the effect of finite size of the atom and all the possible contribution of allowed multipole radiations. The emission process is then analyzed by the quantum stochastic trajectory approach. The non-Markovian effect is counted in by expanding the original system to an enlarged system with Markovian reservoirs. In the case of a hydrogenlike atom with large atomic number Z, the deviation from the Weisskopf-Wigner result is quite evident.

I. INTRODUCTION

The spontaneous emission of an excited two-level atom is an old question in quantum theory. In the year 1930, Weisskopf and Wigner [1] in their investigation of atomic spectra connected a Lorentzian line profile with exponential decay of an upper-level population of the atom. In the following, we shall call the exponential decay with the Einstein A coefficient as decay rate the Weisskopf-Wigner result. Agarwal [2] and Ackerhalt and Eberly [3] presented a fully quantum-electrodynamic treatment of the spontaneous emission with the aid of the Markov approximation. Agarwal worked on the master equation of the atom density operator, while Ackerhalt and Eberly did their calculation in the Heisenberg picture. Both calculations resulted in the Weisskopf and Wigner exponential decay. However, the exponential decay is not necessarily true in general. For stronger coupling, as in the case of a hydrogenlike atom with large atomic number Z, the instaneous decay rate may depend on the history of the process and hence the process is non-Markovian. Moreover, neglecting the finite atom-size effect and restriction to electric dipole transitions may also become improper.

Carrazana and Vetri [4] studied non-Markovian effects in the spontaneous decay of the atomic population difference in 1980. They first derived a master equation for the spontaneous emission process without the Markov approximation, and then arrived at a closed equation for $\langle \hat{\sigma}_3(t) \rangle$, the population difference, in the Born approximation and in the rotating-wave approximation. This equation was studied subsequently by means of the Laplace transformation. But in their approach the atom is actually taken as a pointlike electric dipole, so that the finite-size effect and all higher allowed multipole contributions are neglected; in addition, a cutoff

wavelength was introduced to avoid divergence of the integral with respect to the wave vector. In their numerical calculation the ratio γ_A / ω_0 is taken as large as 0.1, where ω_0 is the atomic transition frequency and γ_A is the corresponding Einstein A coefficient. For such a large value of γ_A / ω_0, apart from its lack of reality, the restriction to the pointlike electric dipole transition, as we show in the following, is irrelevant.

In the 1990s, a kind of new method known as the quantum stochastic trajectory approach [5] and other related stochastic wave equation approaches were developed [6–8] to treat the open system. In this paper the stochastic trajectory formulation will be adopted, in which the solution of the master equation is first expressed as a sum of various possible quantum trajectories [5], and then this summation is calculated by a type of Monte Carlo treatment, namely, the summation is transformed to the ensemble average of so-called stochastic quantum trajectories. This approach has been applied to wide classes of problems. However, its application to a strongly interacting system is seriously limited by its Markov approximation.

A few years ago, Imamoglu and co-workers developed a procedure [9,10] to extend the application range of the stochastic approach to a large class of non-Markovian processes. Their procedure is based on the recognition that a given non-Markovian process of certain type can be embodied in an enlarged Markovian process. Specifically, the original system is expanded by introducing additional fictitious harmonic oscillators which interact on the one hand with the original system and on the other hand with their own reservoirs of vanishing correlation time, namely the enlarged system has Markovian reservoirs. It is well known that the pair of conjugate operators of a harmonic oscillator interacting with a Markovian reservoir will correlate with each other by a finite interval of order of their decay time; hence they will serve as effective non-Markovian reservoirs to the original system they couple with. Through proper selection of the parameters for the fictitious oscillators one may simulate the original non-Markovian reservoirs by these effective alternatives.

There is another stochastic wave function method that is

---

*Email address: cqcao@pku.edu.cn

[†]Present address: Department of Physics, Purdue University, West Lafayette, IN 47907.

[‡]Email address: h-cao@northwestern.edu

also capable of treating a non-Markovian process in a systematic way [11]. The proposed stochastic unraveling is based on a description of the system in a doubled Hilbert space. Non-Markovian effects in the dynamics are then treated by employing the time-convolutionless projection operator technique.

In this paper we shall adopt the former non-Markovian approach, since we find that it is possible to simulate the non-Markovian reservoir in our problem by just a few fictitious oscillators, which makes the numerical task rather easy.

The non-Markovian approach is known to be essential for describing the dissipative dynamics of electrons or excitons in semiconductors. Now we will show that even in the spontaneous emission of a hydrogenlike atom with large atomic number Z the deviation from Weisskopf-Wigner decay is also evident.

The first important thing for this investigation is then to derive the non-Markovian spectrum $R(\omega)$ of the correlation functions for atomic spontaneous emission. We shall do this without the pointlike electric dipole transition approximation. Then the quantum stochastic trajectory approach is used to study the non-Markovian correction to the decay of the atom upper-level population. No cutoff wavelength is needed in our formulation. In the case of "allowed transition," we see that corrections actually come from two factors. The first is the difference between $2\pi R(\omega_0)$ and the Einstein A coefficient γ_A, which means that, if one still makes the Markov approximation but on the basis of the real correlation spectrum, the resultant exponential decay is still quite different from the Weisskopf-Wigner result. The second factor is the nonwhiteness of $R(\omega)$, namely, its deviation from $R(\omega_0)$.

II. THE REAL SPECTRUM OF THE CORRELATION FUNCTION FOR SPONTANEOUS EMISSION OF A TWO-LEVEL ATOM

The $\mathbf{A}\cdot\mathbf{P}$ type $\hat{H}_{int}$ for the spontaneous emission of a two-level atom in the rotating-wave approximation is known to be

$$\hat{H}_{int}(t)=i\hbar\sum_{\mathbf{k},j}\left[g_{\mathbf{k}j}\hat{\sigma}_+(t)\hat{a}_{\mathbf{k}j}(t)-g_{\mathbf{k}j}^*\hat{\sigma}_-(t)\hat{a}_{\mathbf{k}j}^\dagger(t)\right]\quad(1)$$

where $\hat{a}_{\mathbf{k}j}$ ($\hat{a}_{\mathbf{k}j}^\dagger$) is the photon annihilation (creation) operator of mode $(\mathbf{k},j)$, and $\hat{\sigma}_\pm$ are atom-level change operators ($\hat{\sigma}_+$ corresponds to upward change and $\hat{\sigma}_-$ to downward change). For a hydrogenlike atom $g_{\mathbf{k}j}$ is given by

$$g_{\mathbf{k}j}=-\frac{e}{m}\sqrt{\frac{2\pi\hbar}{Vkc}}\boldsymbol{\varepsilon}_{\mathbf{k}j}\cdot\mathbf{G}_\mathbf{k},$$

$$\mathbf{G}_\mathbf{k}=\int e^{i\mathbf{k}\cdot\mathbf{x}}\Psi_2^\dagger(\mathbf{x})\boldsymbol{\nabla}\Psi_1(\mathbf{x})d^3\mathbf{x},\quad(2)$$

in which $\boldsymbol{\varepsilon}_{\mathbf{k}j}$ is the polarization vector of photon mode $(\mathbf{k},j)$, and $\Psi_2(\mathbf{x})$ and $\Psi_1(\mathbf{x})$ are the upper-level and lower-level wave functions, respectively. The dynamical equations for both atom and photon variables are easily deduced from

$\hat{H}_{int}$. Eliminate the operators $\hat{a}_{\mathbf{k}j}$ and $\hat{a}_{\mathbf{k}j}^\dagger$ by taking the electromagnetic (e.m.) fields as reservoir; the resultant differential-integral equations are

$$\frac{d}{dt}\hat{\sigma}_-(t)=\int_0^t u(t-t')\hat{\sigma}_3(t)\hat{\sigma}_-(t')dt'-\hat{\sigma}_3(t)\hat{\Sigma}(t),$$
$$(3a)$$

$$\frac{d}{dt}\hat{\sigma}_3(t)=-2\int_0^t u(t-t')\hat{\sigma}_+(t)\hat{\sigma}_-(t')dt'+2\hat{\sigma}_+(t)\hat{\Sigma}(t)$$

$$+\text{H.c.},\quad(3b)$$

where $\hat{\sigma}_3$ is the atom population-difference operator, and

$$\hat{\Sigma}(t)=\sum_{\mathbf{k}j}g_{\mathbf{k}j}\hat{a}_{\mathbf{k}j}(0)e^{-i(\omega-\omega_0)t}\quad(3c)$$

is the fluctuation force operator.

The correlation function in the above differential-integral equations is expressed by

$$u(t-t')=\sum_{\mathbf{k}j}|g_{\mathbf{k}j}|^2 e^{-i(\omega-\omega_0)(t-t')}$$

$$\equiv\int_0^\infty R(\omega)e^{-i(\omega-\omega_0)(t-t')}d\omega,\quad(4a)$$

in which

$$R(\omega)=\frac{V}{(2\pi)^3}\frac{\omega^2}{c^3}\int d\Omega_k\sum_j|g_{\mathbf{k}j}|^2=\frac{e^2\hbar\omega}{4\pi^2 m^2 c^3}\int d\Omega_k[|G_\mathbf{k}|^2$$

$$-|\mathbf{n}_\mathbf{k}\cdot\mathbf{G}_\mathbf{k}|^2].\quad(4b)$$

In the case of spontaneous emission, $\langle\hat{a}_{\mathbf{k}j}(0)\hat{a}_{\mathbf{k}'j'}^\dagger(0)\rangle_R=\delta_{kk'}\delta_{jj'}$ and all other pairs have zero expectation value; hence no additional correlation function will stem from the fluctuation force.

If the Markov approximation is made on the real spectrum $R(\omega)$, the correlation function will reduce to

$$u(t-t')=(\gamma+i2\delta\omega_0)\delta(t-t').\quad(5a)$$

From Eq. (4a) one may obtain that the value of γ is given by

$$\gamma=2\pi R(\omega_0).\quad(5b)$$

Physically, γ represents the whole transition rate contributed by all allowed multipole (including dipole) radiations and with finite atom size effect included; taking $\omega=\omega_0$ means that the photon energy is equal to the energy difference of the atomic levels. $\delta\omega_0$ represents the frequency shift of the atom level, but its value obtained by our simple model has no meaning and hence it will be omitted.

Correspondingly,

$$\langle\hat{\Sigma}(t)\hat{\Sigma}^\dagger(t')\rangle=\gamma\delta(t-t').\quad(5c)$$

In this case one still obtains exponential decay of the upper-level population $\langle \hat{N}_2(t) \rangle$, but the decay constant is γ, not the Einstein A coefficient γ_A. The latter represents the transition rate contributed by pointlike electric dipole radiation.

In the usual estimation, the characteristic correlation time of $u(t-t')$ is of order $2\pi/\omega_0$ while the decay time of atomic variables is of order $1/\gamma$; hence for the Markov approximation to be valid $2\pi/\omega_0$ should be much less than $1/\gamma$, namely, $2\pi\gamma/\omega_0 \ll 1$. More precise information can only be learned from the solution of the differential-integral equations (3a) and (3b) or of an equivalent master equation.

As a first step we calculate the coupling constant $g_{\mathbf{k}j}$. For simplicity, we omit the spin of the electron. Substituting the wave function

$$\Psi_1(\mathbf{x}) = f_1(r) Y_{l_1 m_1}(\theta\varphi), \qquad \Psi_2(\mathbf{x}) = f_2(r) Y_{l_2 m_2}(\theta\varphi)$$

and also the expansion formula

$$e^{i\mathbf{k}\cdot\mathbf{x}} = 4\pi \sum_{lm} i^l j_l(kr) Y_{lm}(\theta_k\varphi_k) Y_{lm}^*(\theta\varphi) \qquad (6)$$

into Eq. (2) and making use of the formula

$$\nabla\Psi_1(\mathbf{x}) = -\sqrt{\frac{l_1+1}{2l_1+1}}\left[\frac{df_1(r)}{dr} - \frac{l_1}{r}f_1(r)\right]\mathbf{T}_{l_1 l_1+1 m_1}(\theta\varphi)$$
$$+ \sqrt{\frac{l_1}{2l_1+1}}\left[\frac{df_1(r)}{dr} + \frac{l_1+1}{r}f_1(r)\right]$$
$$\times \mathbf{T}_{l_1 l_1-1 m_1}(\theta\varphi), \qquad (7)$$

where $\mathbf{T}_{jlm}(\theta\varphi)$ is the vector harmonics, one gets $\mathbf{G}_\mathbf{k}$ after integration over θ_k, φ_k:

$$\mathbf{G}_\mathbf{k} = (-1)^{m_2}\sqrt{\frac{4\pi(2l_2+1)}{2l_1+1}}\sum_{lm\mu}\frac{i^l}{\sqrt{2l+1}}Y_{lm}(\theta_k\varphi_k)[-\sqrt{(l_1+1)(2l_1+3)}\{A_l(\omega) - l_1 B_l(\omega)\}C(l_1+1,1,l_1;m_1$$
$$-\mu,\mu,m_1)C(l_1+1,l_2,l;m_1-\mu,-m_2,m)C(l_1+1,l_2,l;0,0,0) + \sqrt{l_1(2l_1-1)}\{A_l(\omega) + (l_1+1)B_l(\omega)\}$$
$$\times C(l_1-1,1,l_1;m_1-\mu,\mu,m_1)C(l_1-1,l_2,l;m_1-\mu,-m_2,m)C(l_1-1,l_2,l;0,0,0)]\mathbf{n}_\mu, \qquad (8a)$$

in which $C(l_1+1,1,l_1;m_1-\mu,\mu,m_1)$, etc., are Clebsch-Gordan coefficients, $\mathbf{n}_\mu$ ($\mu = +1,0,-1$) are spherical bases

$$\mathbf{n}_{+1} = -\frac{1}{\sqrt{2}}(\mathbf{n}_1 + i\mathbf{n}_2), \qquad \mathbf{n}_0 = \mathbf{n}_3, \qquad \mathbf{n}_{-1} = \frac{1}{\sqrt{2}}(\mathbf{n}_1 - i\mathbf{n}_2)$$
$$(8b)$$

satisfying the relations

$$\mathbf{n}_\mu^* = (-1)^\mu \mathbf{n}_{-\mu}, \qquad \mathbf{n}_\mu^* \cdot \mathbf{n}_{\mu'} = \delta_{\mu\mu'},$$

and

$$A_l(\omega) = \int_0^\infty r^2 j_l\left(\frac{\omega}{c}r\right)f_2(r)\frac{df_1(r)}{dr}dr, \qquad (8c)$$

$$B_l(\omega) = \int_0^\infty r j_l\left(\frac{\omega}{c}r\right)f_2(r)f_1(r)dr. \qquad (8d)$$

The summation in Eq. (8a) actually contains only finite terms because of the angular momentum addition rule. For the first term in the square brackets, l is restricted to the range $|l_2 - l_1 - 1| \leq l \leq l_2 + l_1 + 1$, and for the second term to the range $|l_2 - l_1 + 1| \leq l \leq l_2 + l_1 - 1$. Substituting $\mathbf{G}_\mathbf{k}$ and the formula

$$\mathbf{n}_\mathbf{k} = \sqrt{\frac{4\pi}{3}}\sum_\mu Y_{l\mu}(\theta_k\varphi_k)\mathbf{n}_\mu^* \qquad (9)$$

into Eq. (4b) and carrying out the integration over θ_k and φ_k, one may obtain the spectral function $R(\omega)$ immediately.

To see these spectral functions explicitly, we consider a simple example. $\Psi_1(\mathbf{x})$ and $\Psi_2(\mathbf{x})$ are Schrödinger wave functions with quantum numbers $(n_1=1, l_1=0)$ and $(n_2=2, l_2=1, m_2=1)$, respectively, expressed by

$$\Psi_1(\mathbf{x}) = \frac{1}{\sqrt{4\pi}}N_1 e^{-r/a_1}, \qquad N_1 = \sqrt{\frac{4}{a_1^3}}, \qquad (10a)$$

$$\Psi_2(\mathbf{x}) = N_2 r e^{-r/a_2}Y_{11}(\theta\varphi), \qquad N_2 = \sqrt{\frac{4}{3a_2^5}}. \qquad (10b)$$

The corresponding transition is an allowed transition, so we can compare our result with that of Weisskopf and Wigner. In this simple case, the gradient of $\Psi_1(\mathbf{x})$ is given by

$$\nabla\Psi_1(\mathbf{x}) = -\frac{1}{\sqrt{4\pi}}N_1\frac{1}{a_1}e^{-r/a_1}\mathbf{n}_\mathbf{r} \qquad (11)$$

where $\mathbf{n}_\mathbf{r}$ is the unit vector along $\mathbf{r}$ and is expressed in the spherical bases as

$$\mathbf{n}_\mathbf{r} = \sqrt{\frac{4\pi}{3}}\sum_\mu (-1)^\mu Y_{l\mu}(\theta\varphi)\mathbf{n}_{-\mu}, \qquad \mu = +1,0,-1.$$
$$(12)$$

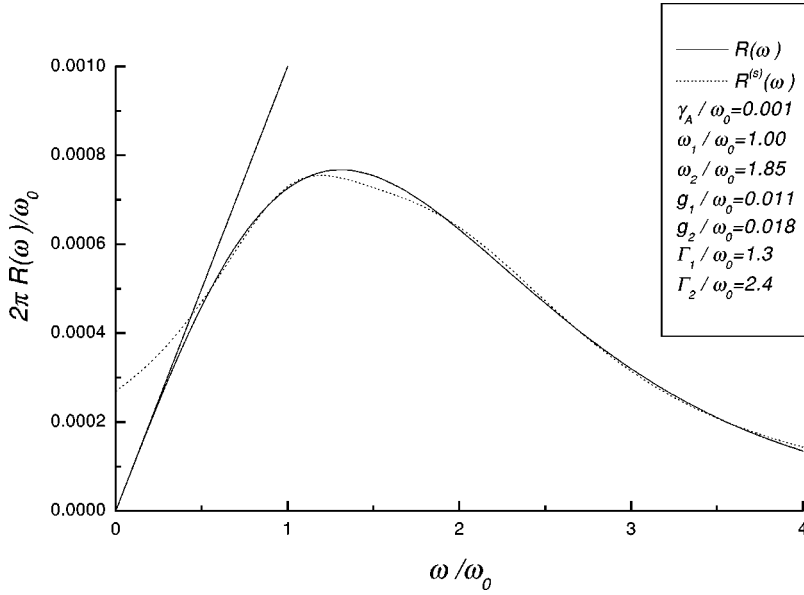Substituting these formulas and Eq. (6) into Eq. (2) and carrying out the angular integration, one obtains

FIG. 1. Simulation of real correlation spectrum by two Lorentzian spectral profiles. The straight line represents the point-electric-dipole spectrum $R^D(\omega)$.

$$\mathbf{G_k} = \sqrt{\frac{4\pi}{3}} \frac{N_1 N_2}{a_1} \left[X_0(\omega) Y_{00}(\theta_k \varphi_k) \mathbf{n}_{-1} + X_2(\omega) \right.$$

$$\times \left(\sqrt{\frac{6}{5}} Y_{2,-2}(\theta_k \varphi_k) \mathbf{n}_{+1} - \sqrt{\frac{3}{5}} Y_{2,-1}(\theta_k \varphi_k) \mathbf{n}_0 \right.$$

$$\left. \left. + \sqrt{\frac{1}{5}} Y_{2,0}(\theta_k \varphi_k) \mathbf{n}_{-1} \right) \right] \tag{13a}$$

where

$$X_0(\omega) = \int_0^\infty r^3 j_0\left(\frac{\omega}{c} r\right) e^{-r/a} dr = \frac{2a^4(3 - \omega^2 a^2/c^2)}{(1 + \omega^2 a^2/c^2)^3}, \tag{13b}$$

$$X_2(\omega) = \int_0^\infty r^3 j_2\left(\frac{\omega}{c} r\right) e^{-r/a} dr = \frac{8a^4 \omega^2 a^2/c^2}{(1 + \omega^2 a^2/c^2)^3}. \tag{13c}$$

with

$$\frac{1}{a} = \frac{1}{a_1} + \frac{1}{a_2}. \tag{13d}$$

Both $A_l(\omega)$ and $B_l(\omega)$ are proportional to $X_l(\omega)$.

The spectrum $R(\omega)$ is then calculated straightforwardly with the result

$$R(\omega) = \frac{\gamma_A}{2\pi\omega_0} \frac{\omega}{(1 + \omega^2 a^2/c^2)^4}, \tag{14a}$$

in which γ_A is the Einstein A coefficient, given by

$$\gamma_A = \frac{4\omega_0^3 |d_{21}|^2}{3c^3 \hbar}, \tag{14b}$$

and in our example the transition dipole moment $\mathbf{d}_{21}$ takes its absolute value as

$$|d_{21}| = 64 \sqrt{\frac{2}{81}} ae \cong 1.12 ae \tag{14c}$$

with e denoting the magnitude of the electronic charge.

Actually there is only one parameter in $R(\omega)$, since ω_0 may also be expressed in terms of a as

$$\omega_0 = \frac{1}{\hbar}(E_2 - E_1) = \frac{\hbar}{6ma^2}. \tag{15}$$

The two atomic radii a_1 and a_2 in our example are related to a by simple numerical constants:

$$a_1 = \frac{3}{2}a, \quad a_2 = 3a. \tag{16}$$

A profile of $R(\omega)$ is shown in Fig. 1, in which the parameter in $R(\omega)$ is taken as $\gamma_A/\omega_0 = 0.001$; for discussion see below.

In the literature [4], the atom with an allowed transition is taken as a pointlike electric dipole in the calculation of the correlation spectra, so that the factor $e^{i\mathbf{k} \cdot \mathbf{x}}$ in $\mathbf{G_k}$ is omitted. $\mathbf{G_k}$ is then independent of $\mathbf{k}$; hence the correlation spectrum becomes linear in ω, as can be seen from Eq. (4b). For such a pointlike atom, the $R(\omega)$ in Eq. (14a) will reduce to

$$R^D(\omega) = \frac{\gamma_A}{2\pi\omega_0} \omega, \tag{17}$$

corresponding to letting $\omega a/c = 0$. This formula actually holds for more general $\Psi_1(\mathbf{x})$ and $\Psi_2(\mathbf{x})$, since

$$\mathbf{G_k^D} = \int \Psi_2^*(\mathbf{x}) \nabla \Psi_1(\mathbf{x}) d^3 x = \frac{m}{e\hbar} \omega_0 \mathbf{d}_{21}, \tag{18}$$

which leads to Eq. (17) after substituting in Eq. (4b). In the following we shall call $R^D(\omega)$ the point-electric-dipole spec-

trum; it neglects the contributions of all higher multipole moments as well as the finite-size effects.

Quantitatively, we see from Eq. (14a) that in the range

$$\frac{\omega a}{c} < 0.05 \tag{19}$$

the spectrum $R(\omega)$ almost coincides with $R^D(\omega)$ with errors less than 1%. To see whether ω_0 lies in this range, we rewrite Eq. (15) as

$$\frac{\omega_0 a}{c} = \frac{1}{6} \frac{e^2}{\hbar c} \frac{r_B}{a} = \frac{1}{4} \frac{Z e^2}{\hbar c} \tag{20}$$

where $e^2/\hbar c$ is the fine structure constant and r_B is the Bohr radius $\hbar^2/m e^2$. Hence $R^D(\omega)$ will be valid up to cover the point ω_0, provided

$$\frac{a}{r_B} > \frac{10}{3} \frac{e^2}{\hbar c} \quad (\approx 2.4 \times 10^{-2}). \tag{21}$$

We see that $R^D(\omega)$ shoots up in Fig. 1 while the finite size of the atom makes $R(\omega)$ drop down. The maximum value of $R(\omega)$ appears at

$$\omega_{max} = \frac{c}{\sqrt{7} a}. \tag{22}$$

When $\omega^2 \gg c^2/a^2$, $R(\omega)$ rapidly descends as ω^{-7}. Roughly speaking the effect of finite atom size is to cut off the point-electric-dipole spectrum at a value of about c/a. The underlying physics is evident: when the e.m. wavelength λ becomes comparable with or smaller than the atom diameter $2a$, the phase of the e.m. wave will oscillate over a range of 2π or even more within the electron cloud, leading to partly positive and partly negative coupling of the electron to the e.m. wave. It is this kind of cancellation that finally results in a dying away of the total coupling.

Another important quantity for allowed transition is γ_A/ω_0. It is expected that if a neighborhood around ω_0 with an extent of a few γ_A wholly lies within the range denoted by Eq. (19), the point-electric-dipole spectrum $R^D(\omega)$ can be substituted for the real spectrum $R(\omega)$ in the spontaneous emission problem. We see the case shown in Fig. 1 is completely not of this kind.

From Eqs. (14b) and (14c), one gets

$$\frac{\gamma_A}{\omega_0} = \frac{8}{3} \left(\frac{64}{81} \right)^2 \frac{e^2}{\hbar c} \left(\frac{\omega_0 a}{c} \right)^2 \cong 1.22 \times 10^{-2} \left(\frac{\omega_0 a}{c} \right)^2. \tag{23}$$

We shall taken this dimensionless parameter instead of a to mark the $R(\omega)$, as we already have in Fig. 1. The value $\gamma_A/\omega_0 = 10^{-3}$ corresponds to $Z \simeq 157$, somewhat larger than the upper limit of real nuclei.

III. QUANTUM STOCHASTIC TRAJECTORY APPROACH TO THE SPONTANEOUS EMISSION

We have shown that the two-level atom in general has a non-Markovian reservoir in its spontaneous emission. Hence we will, as described in Sec. I, introduce N additional fictitious harmonic oscillators, which interact with the atom in the same form as photons, to form the expanded system. This expanded system thus has the Hamiltonian

$$\hat{H} = \frac{1}{2} \hbar \omega_0 \hat{\sigma}_3 + \sum_{j=1}^{N} \hbar \omega_j \hat{\alpha}_j^\dagger \hat{\alpha}_j + i\hbar \sum_{j=1}^{N} (g_j \hat{\sigma}_+ \hat{\alpha}_j - g_j^* \hat{\sigma}_- \hat{\alpha}_j^\dagger), \tag{24}$$

in which the energies of the two atom levels are taken as $\pm \frac{1}{2} \hbar \omega_0$, respectively, and $\hat{\alpha}_j$ and $\hat{\alpha}_j^\dagger$ are the annihilation and creation operators of the jth oscillator. Each of these oscillators, on the other hand, is assumed to interact with its own reservoir with no memory; hence the expanded system is Markovian. In terms of Langevin equations in the Heisenberg picture the above concept is expressed as

$$\frac{d}{dt} \hat{\sigma}_-(t) = -i\omega_0 \hat{\sigma}_-(t) - \sum_{j=1}^{N} g_j \hat{\alpha}_j(t) \hat{\sigma}_3(t), \tag{25a}$$

$$\frac{d}{dt} \hat{\sigma}_3(t) = 2 \sum_{j=1}^{N} g_j \hat{\alpha}_j(t) \hat{\sigma}_+(t) + 2 \sum_{j=1}^{N} g_j^* \hat{\alpha}_j^\dagger(t) \hat{\sigma}_-(t), \tag{25b}$$

$$\frac{d}{dt} \hat{\alpha}_j(t) = -i\omega_j \hat{\alpha}_j(t) - g_j^* \hat{\sigma}_-(t) - \frac{1}{2} \Gamma_j \hat{\alpha}_j(t) - \hat{F}_j(t) \tag{25c}$$

with

$$\langle \hat{F}_j(t) \rangle_R = 0, \quad \langle \hat{F}_i(t) \hat{F}_j^\dagger(t') \rangle_R = \delta_{ij} \Gamma_j \delta(t - t'),$$

$$\langle \hat{F}_i(t) \hat{F}_j(t') \rangle_R = 0. \tag{25d}$$

The last two terms of Eq. (25c) are the usual Markovian dissipation term and fluctuation term contributed by the reservor of the jth oscillator.

When the formal solution of Eq. (25c) is used to eliminate the variables $\hat{\alpha}_j$ and $\hat{\alpha}_j^\dagger$ in Eqs. (25a) and (25b), the reduced equation for $\hat{\sigma}_+(t)$ and $\hat{\sigma}_3(t)$ will have non-Markovian damping terms and non-Markovian fluctuation terms since each fictitious oscillator contributes a term with a Lorentzian type spectrum. The next step is to select parameters g_j, ω_j, and Γ_j to simulate the original damping and fluctuation terms.

As soon as the simulation task is accomplished, one may go back to the master-equation formulation and treat it by the quantum stochastic trajectory approach. The non-Hermitian Hamiltonian is now taken as

$$\hat{H}_{nh} = \hat{H} - \frac{i}{2} \hbar \sum_j \Gamma_j \hat{\alpha}_j^\dagger \hat{\alpha}_j, \tag{26}$$

where $\hat{H}$ is expressed by Eq. (24). The collapse operators acting on $|\Psi(t)\rangle$ are
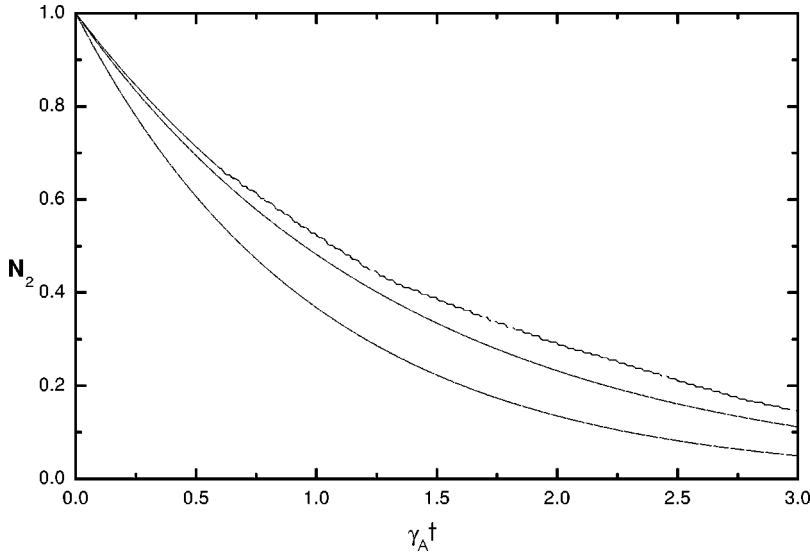
FIG. 2. The spontaneous decay of the upper-level population with parameters $\gamma_A/\omega_0 = 1 \times 10^{-3}$, $\omega_{max}/\omega_0 \approx 1.32$. The upper line represents the result without Markov approximation, the middle line represents the result with the Markov approximation to the real spectrum $R(\omega)$, and the lowest line represents the Weisskopf-Wigner result.

$$\hat{C}_j = \sqrt{\Gamma_j \Delta t}\,\hat{\alpha}_j, \qquad j = 1,2,\ldots,N. \qquad (27)$$

To proceed with a concrete analysis, we return to the simple example with $\Psi_2(\mathbf{x})$ and $\Psi_1(\mathbf{x})$ described by Eqs. (10), and try to introduce just two fictitious oscillators to simulate $R(\omega)$, namely, to express $R(\omega)$ approximately by $R^{(s)}(\omega)$ contributed by two fictitious oscillators:

$$R^{(s)}(\omega) = \frac{1}{2\pi} \sum_{j=1}^{2} \frac{|g_j|^2 \Gamma_j}{(\omega - \omega_j)^2 + \frac{1}{4}\Gamma_j^2}. \qquad (28)$$

Before starting the simulation, we should first set the value of the parameter in $R(\omega)$ which is now taken as γ_A/ω_0 as mentioned below Eq. (23). For the hydrogen atom, $\gamma_A/\omega_0 \approx 4 \times 10^{-8}$ and $\omega_0/\omega_{max} \approx 5 \times 10^{-3}$; thus in this case one may use $R^D(\omega)$ to replace $R(\omega)$ and the non-Markovian correction is negligible. When the atomic number Z increases, the radii a_1, a_2, and a decrease as $1/Z$. Hence γ_A/ω_0 is proportional to Z^2 as can be seen from Eqs. (15) and (23). The largest realistic value of Z is about 10^2; thus

γ_A/ω_0 may approach 4×10^{-4}, which is of the same order of the γ_A/ω_0 we take in the $R(\omega)$ of Fig. 1.

We see from Fig. 1 that by properly choosing the parameters ω_j, g_j, and Γ_j ($j = 1,2$) the $R^{(s)}(\omega)$ of Eq. (26) indeed fits $R(\omega)$ quite well, except in the very low frequency region. In addition, at the point around $\omega = \omega_0$, $R(\omega)$ is quite different from the point-electric-dipole spectrum $R^D(\omega)$, and ω_0 is not far from ω_{max}. Actually from Eqs. (22) and (23), ω_{max}/ω_0 takes a value about 1.32 for $\gamma_A/\omega_0 = 10^{-3}$.

Since the numerical evolution takes place over discrete times with a small time step Δt, the wave function $|\Psi(t)\rangle$ is represented by a sequence $|\Psi(t_n)\rangle$ with $t_n = n\Delta t$. Given the value of $|\Psi(t_n)\rangle$, the next one $|\Psi(t_{n+1})\rangle$ is determined by the following algorithm.

(1) Evaluate the two collapse probabilities during the interval (t_n, t_{n-1}):

$$P_1(t_n) = \langle \Psi(t_n)|\hat{C}_1^\dagger \hat{C}_1|\Psi(t_n)\rangle = \Gamma_1 \langle \Psi(t_n)|\hat{\alpha}_1^\dagger \hat{\alpha}_1|\Psi(t_n)\rangle \Delta t,$$
$$(29a)$$

$$P_2(t_n) = \langle \Psi(t_n)|\hat{C}_2^\dagger \hat{C}_2|\Psi(t_n)\rangle = \Gamma_2 \langle \Psi(t_n)|\hat{\alpha}_2^\dagger \hat{\alpha}_2|\Psi(t_n)\rangle \Delta t,$$
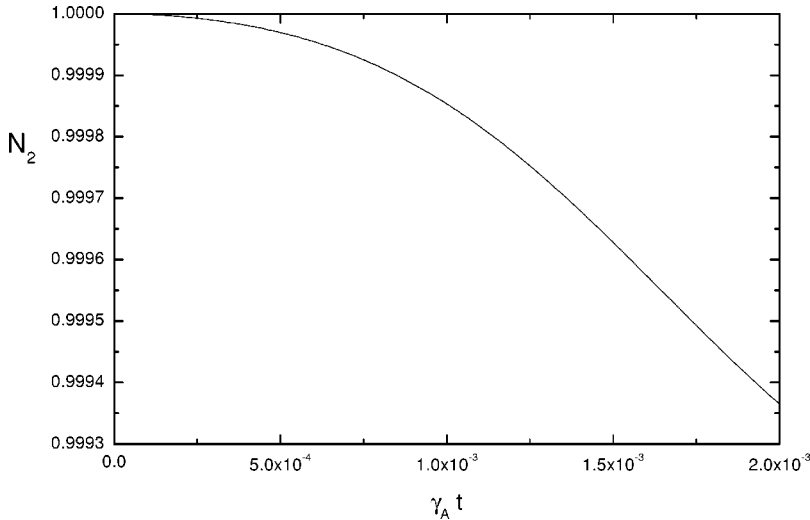$$(29b)$$

FIG. 3. The initial stage of evolution of the upper-level population with the real correlation spectrum ($\gamma_A/\omega_0 = 1 \times 10^{-3}$, $\omega_{max}/\omega_0 \approx 1.32$).
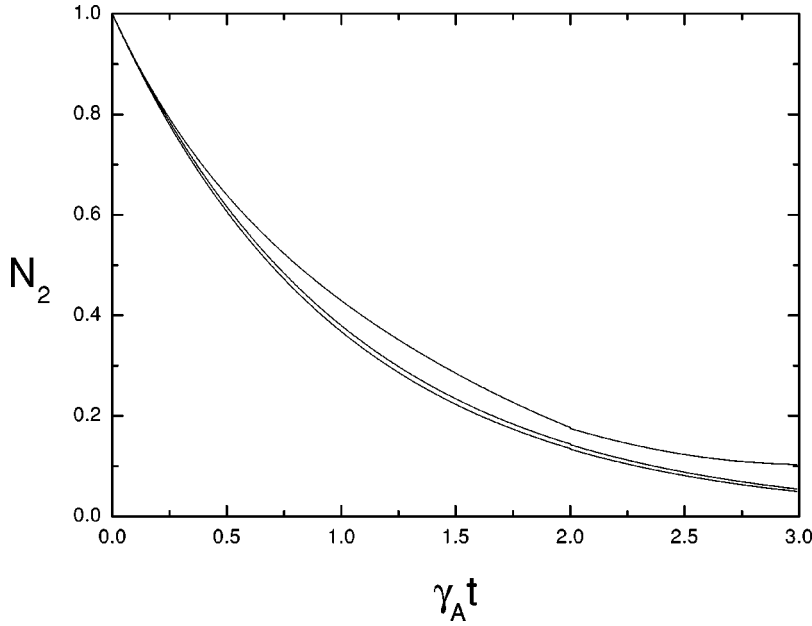
FIG. 4. The spontaneous decay of the upper-level population with $Z \cong 50$ ($\gamma_A/\omega_0 = 1 \times 10^{-4}$). The upper line is without Markov approximation, the middle one represents the result with the Markov approximation to the real spectrum, and the lowest one represents the Weisskopf-Wigner result.

where Δt should be small enough to make $P_1(t_n)$ and $P_2(t_n)$ much smaller than 1.

(2) Generate two random numbers r_1 and r_2 which have uniform probability distribution in the interval (0,1).

(3) Compare $P_1(t_n)$, and $P_2(t_n)$ with r_1, and r_2 and derive $|\Psi(t_{n+1})\rangle$ according to the following rule:

$$|\Psi(t_{n+1})\rangle = \frac{\hat{C}_1|\Psi(t_n)\rangle}{\sqrt{\langle\Psi(t_n)|\hat{C}_1^\dagger\hat{C}_1|\Psi(t_n)\rangle}}$$

if $P_1(t_n) > r_1$ and $P_2(t_n) \leq r_2$,

$$|\Psi(t_{n+1})\rangle = \frac{\hat{C}_2|\Psi(t_n)\rangle}{\sqrt{\langle\Psi(t_n)|\hat{C}_2^\dagger\hat{C}_2|\Psi(t_n)\rangle}}$$

if $P_1(t_n) \leq r_1$ and $P_2(t_n) > r_2$,

$$|\Psi(t_{n+1})\rangle = \frac{\hat{C}_2\hat{C}_1|\Psi(t_n)\rangle}{\sqrt{\langle\Psi(t_n)|\hat{C}_1^\dagger\hat{C}_2^\dagger\hat{C}_2\hat{C}_1|\Psi(t_n)\rangle}}$$

if $P_1(t_n) > r_1$ and $P_2(t_n) > r_2$,

$$|\Psi(t_{n+1})\rangle = \frac{e^{-i/\hbar\hat{H}_{nh}\Delta t}|\Psi(t_n)\rangle}{\sqrt{\langle\Psi(t_n)|e^{i/\hbar(\hat{H}_{nh}^\dagger - \hat{H}_{nh})\Delta t}|\Psi(t_n)\rangle}}$$
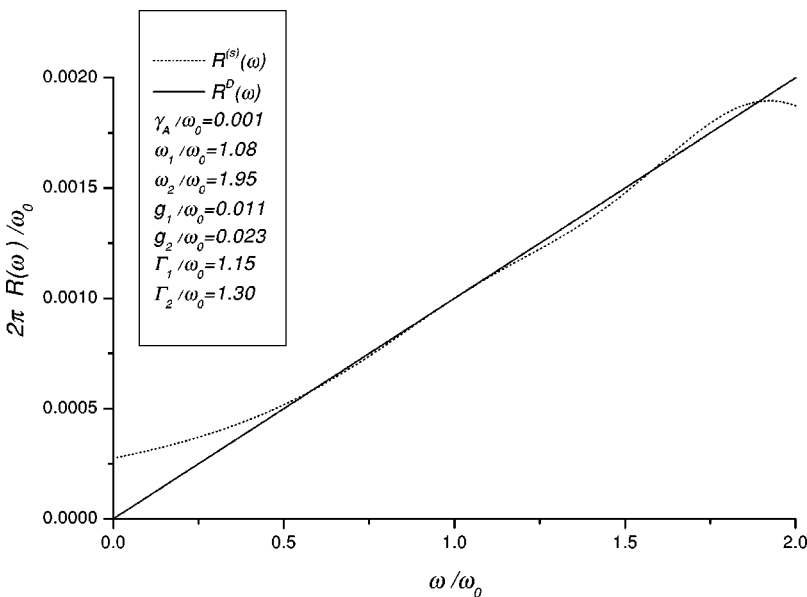
if $P_1(t_n) < r_1$ and $P_2(t_n) < r_2$.

FIG. 5. Simulation of point-electric-dipole spectrum by two Lorentzian spectral profiles. $R^D(\omega)$ is the point-electric-dipole spectrum, $R^{(s)}(\omega)$ is its simulation.
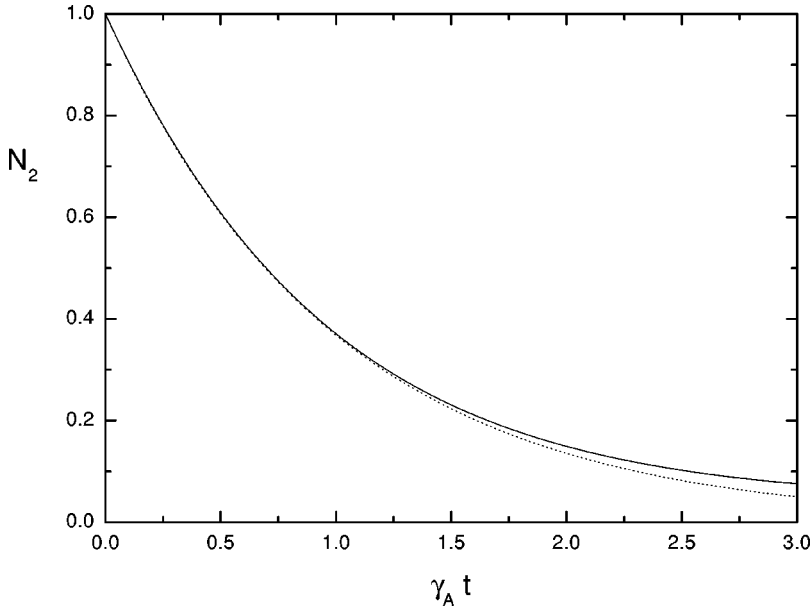
FIG. 6. The spontaneous decay of the upper-level population according to the point-electric-dipole spectrum ($\gamma_A/\omega_0 = 1 \times 10^{-3}$). The solid line is without the Markov approximation, and the dotted one is with the Markov approximation, which is now identical to the Weisskopf-Wigner result.

By carrying out the steps specified above repeatedly from the initial state $\binom{1}{0}|0,0\rangle$ where $\binom{1}{0}$ is the atom state in the upper level and $|0,0\rangle$ denotes the state of two oscillators with both particle numbers being zero, we get a quantum stochastic trajectory of the Monte Carlo wave function $|\Psi(t)\rangle$. The expectation value of a given operator with respect to $|\Psi(t)\rangle$ is then calculated. Finally an ensemble average of 400 trajectories is carried out to give the resultant curve.

The population in the upper level $\langle \hat{N}_2(t) \rangle$ is shown in Fig. 2. We see that the non-Markovian result is quite different from the Weisskopf-Wigner result but not too much different from the result with the Markovian approximation to the real spectrum, in which the decay rate γ is defined by Eq. (5b). One sees from Fig. 2 that at the point $\gamma_A t = 1$ the value of the middle curve is about 0.5, considerably larger than the usual Weisskopf-Wigner value $1/e$. This result can also be expected from Fig. 1: the value of $R(\omega_0)$ is considerably smaller than $R^D(\omega_0)$, while the former equals $\gamma/2\pi$ and the latter equals $\gamma_A/2\pi$.

Carrazana and Vetri [4] pointed out that at the very beginning of the evolution $\langle \hat{N}_2(t) \rangle$ slopes gently with $(d/dt)\langle \hat{N}_2(t)\rangle|_{t=0} = 0$. Figure 2 does not show this behavior because this nearly horizontal part is too short. When we carry out a fine-scale investigation at the very beginning stage, this behavior is clearly shown. We plot this short part in Fig. 3. Actually this result may also be seen from Eq. (3b), since the integrals on the right-hand side tend to zero as $t \rightarrow 0$. If γ_A/ω_0 is taken as a fictitious value 0.01, this characteristic becomes very evident and makes the non-Markovian correction large in the early evolution.

Now we turn to the case of somewhat smaller Z. In the case $\gamma_A/\omega_0 = 1.0 \times 10^{-4}$ (the relevant Z is about 50), the corresponding curve $2\pi R(\omega)/\omega_0$ versus ω/ω_0 keeps the same form as that in Fig. 1, but the scale is changed so that the point $\omega/\omega_0 = 1$ is now located in the initial region with linear behavior. In order to make the simulation spectrum $R^{(s)}(\omega)$ fit $R(\omega)$ down to the neighborhood of the point

$\omega/\omega_0 = 1$, one should introduce more than two fictitious oscillators in $R^{(s)}(\omega)$. Figure 4 represents the corresponding decay of $\langle \hat{N}_2(t) \rangle$ with time; one sees that the Markovian correction is of the same order of magnitude as that in Fig. 2, but the difference between γ and γ_A becomes much smaller.

Lastly, we inspect the non-Markovian effect for point-electric-dipole spectrum. For comparison, the value of γ_A/ω_0 is still taken as 1.0×10^{-3}. We again introduce two fictitious oscillators to expand the system. Figure 5 shows that the point-electric-dipole spectrum can also be fitted quite well with two Lorentzian spectral profiles in the range $\frac{1}{2} < \omega/\omega_0 < 2$. The evolution of N_2 obtained by the quantum stochastic trajectory approach is given by Fig. 6. Now the non-Markovian correction becomes much smaller and is just visible for quite large $\gamma_A t$. This may be the reason why γ_A/ω_0 in Ref. [4] is taken as such a large value as 0.1 to exhibit the non-Markovian effect. We note that now the Markov approximate result in Fig. 6 is identical to the usual Weisskopf-Wigner result since $2\pi R^D(\omega_0) = \gamma_A$. By comparison of Fig. 6 with Fig. 2 we see that the two upper curves for the real spectrum and the point-electric-dipole spectrum, respectively, are also quite obviously different from each other.

IV. BRIEF SUMMARY

We show that the Weisskopf-Wigner result for spontaneous emission of the hydrogenlike atom with allowed transition has quite a large error when the atomic number Z increases to a value of about 50. The error comes from two factors. If we denote the real correlation spectrum of spontaneous emission by $R(\omega)$, the first factor comes from the difference between the Einstein A coefficient γ_A and γ, the $2\pi R(\omega_0)$, which takes into account the finite-size effect and all possible multipole radiation. The second factor comes from the nonwhiteness of the $R(\omega)$, namely, its deviation from $R(\omega_0)$. Both factors make the curve of $N_2(t)$ drop

more slowly. The first correction is calculated analytically in this paper, while the second correction (due to the non-Markov behavior of the correlation spectrum) presented here is calculated numerically and is not so definite, because of simulation error and also the pseudocharacter of the program generated random numbers.

[1] V. Weisskopf and E. Wigner, Z. Phys. **63**, 54 (1930).

[2] G.S.Agarwal, Quantum Optics, Springer Tracts in Modern Physics Vol. 70 (Springer, Berlin, 1974).

[3] J.R. Ackerhalt and J.H. Eberley, Phys. Rev. D **10**, 3350 (1974).

[4] P. Carrazana and G. Vetri, Nuovo Cimento Soc. Ital. Fis., B **55**, 191 (1980).

[5] See, for example, H.J. Carmichael, *An Open System Approach to Quantum Optics*, Lecture Notes in Physics New Series M Vol. 7 (Springer, Berlin, 1993).

[6] J. Dalibard, Y. Castin, and K. Mølmer, Phys. Rev. Lett. **68**, 580 (1992); K. Mølmer, Y. Castin, and J. Dalibard, J. Opt. Soc. Am. B **10**, 524 (1993).

[7] R. Dum, P. Zoller, and H. Ritsch, Phys. Rev. A **45**, 4879 (1992); C.W. Gardiner, A.S. Pakins, and P. Zoller, *ibid.* **46**, 4363 (1992); R. Dum, A.S. Pakins, P. Zoller, and C.W. Gardiner, *ibid.* **46**, 4382 (1992).

[8] N. Gisin and I.C. Percival, J. Phys. A **25**, 5677 (1992).

[9] A. Imamoglu, Phys. Rev. A **50**, 3650 (1994).

[10] P. Stenius and A. Imamoglu, Quantum Semiclassic. Opt. **8**, 283 (1996).

[11] H.-P. Breuer, B. Kappler, and F. Petruccione, Phys. Rev. A **59**, 1633 (1999).